PROCEEDINGS, 48th Workshop on Geothermal Reservoir Engineering
Stanford University, Stanford, California, February 6-8, 2023
SGP-TR-224

Hydrophobic, Thermal Shock-Resistant Latex-Modified Lightweight Class G Cement Composites in Reservoir Thermal Energy Storage (RTES) Systems

Tatiana Pyatina[1], Toshifumi Sugama[1]

[1]Brookhaven National Laboratory

734 Brookhaven Ave. Upton, NY 11973

tpyatina@bnl.gov

Keywords: hydrophobic cement, lightweight cement composite, reservoir thermal energy storage system, latex-modified cement, XSBR latex, geothermal well

ABSTRACT

Energy losses can be significantly reduced if thermally insulating cement is used for energy storage and recovery. The thermal conductivity of the currently used cement is between 1 and 1.2 W/mK. In this study we assessed the ability of polystyrene (PS)-polybutadiene (PB)-polyacrylic acid (PAA) terpolymer (XSBR) latex to improve thermal insulating properties and thermal shock (TS) resistance of class G Ordinary Portland Cement (OPC) and fly ash cenospheres (FCS) composites in the temperature range of 100°-175°C. The composites autoclaved at 100°C were subjected to 3 cycles of TS (one cycle: 175°C heat → 25°C water quenching). In hydrothermal and thermal (TS) environments at elevated temperatures in cement slurries the XSBR latex formed acrylic calcium complexes through acid-base reactions, and the number of such complexes increased at higher temperatures due to the XSBR degradation with formation of additional acrylic groups. As a result, these complexes offered the following five advanced properties to the OPC-based composites: 1) enhanced hydrophobicity; 2) decreased water-fillable porosity; 3) reduced thermal conductivity for water-saturated composites; 4) minimized loss of compressive strength, Young's modulus, and compressive fracture toughness after TS; and 5) abated pozzolanic activity of FCS, which allowed FCS to persist as thermal insulators under strongly alkali conditions of cement slurries. Additionally, XSBR-modified slurries possessed improved workability and decreased slurry density due to the air entraining effect of latex, which resulted in further improvement of thermal insulation performance of the modified composites.

1. INTRODUCTION

In our previous publications we reported design and evaluation of cement composites with very low thermal conductivity (TC) for geothermal energy storage and heat recovery wells (Sugama and Pyatina 2021, 2022). We reported formulation and testing of highly hydrophobic lightweight cement composite with TC of 0.4 – 0.5 W/mK under water-saturated conditions. Such low TC was achieved using hollow Fly Ash Cenospheres (FCS) treated with polymethylhydrosiloxane (PMHS) that tailors chemically the microsphere surfaces making them hydrophobic and providing their stability under alkaline cement environments. The TC of insulating cement composite was further decreased using hydrophobic silica aerogel, which has very high volumetric fraction of air and a surface treatment with hexamethyldisilazane (HMDS). The hydrophobic treatment of HSA particles improves their hydrothermal stability (Koyano et al. 1997; Park et al. 2001; Castricum et al. 2008), protects them from pozzolanic reactions in cement slurries and limits water penetration into the composite, which allows achieving very low TC values.

As a result of that work, combining low strength HSA with FCS and high strength calcium-phosphate cement (CaP) binder allowed improving mechanical properties of composites with very weak HSA particles and reaching very low TC values. The composites were cured at 100 or 250°C and tested in 3 cycles of TS tests with temperature gradients of 150 or 225°C respectively (1 cycle: 175°C heat for 24h → 25°C water quenching for 100°C autoclaved samples and 250°C heat for 24h → 25°C water quenching for 250°C autoclaved samples). Because of the lower pH of CaP cement (pH ~10 in tested blends) than commonly used OPC-based composites (pH ~13), the pozzolanic reactions that lead to the degradation of solid FCS shells, release of the insulating gasses, and the loss of the cement integrity were minimized. The hydrophobic nature of HSA treated with HMDS provided cements with water-repellant properties preventing water ingress and increased TC. The optimized 90/10 FCS/HSA ratio samples after TS tests possessed TC of 0.35 and 0.28 W/mK for 100° and 250°C autoclaved cements, respectively and compressive strength >800 psi (Sugama and Pyatina 2022).

On the other hand, in our work aimed at mitigating the brine-led corrosion of carbon steel (CS) casing by alkali-activated air-foamed lightweight calcium-aluminate-cement sheath, we evaluated the ability of acrylic polymer emulsion containing functional carboxyl (-COOH) and alkyl ester (-COOR) groups to protect CS against corrosion. In the cement slurry cations of calcium, sodium, aluminum, and hydroxide ions, liberated by cement hydration and the activator, formed $(COO^-)_n$-- M^{n+}] complexes (M: Ca, Na, and Al; n: cationic charges of M) with the polymer (Sugama and Pyatina 2013). These derivatives not only offered the improved thermal stability of polymer, but also served in impeding the permeation of corrosive electrolytes through foamed cement, providing cathodic protection of CS against hot brine-caused corrosion. Additionally, in this study, we visually observed the water-repellent behavior of the polymer-modified cement surfaces.

Thus, in this paper we report the use of the carboxylated styrene butadiene rubber (XSBR) latex as terpolymer containing functional carboxyl groups for modifications of class G OPC with FCS for applications in low (100°C) temperature RTES systems. In such systems

cement sheath can encounter significant thermal stresses when hot fluid is pumped into the relatively cold reservoir or when hot fluid is recovered from it passing through the cool upper parts of the well.

To evaluate applicability of XSBR latex for applications in RTES wells we tested thermal shock (TS) resistance (150°C thermal gradient) of 100°C autoclaved cement composites. The work aimed to evaluate possibility of designing hydrophobic insulting TS resistant cement composites. Effects of XSBR latex on OPC hydration at 100°C and 175°C, hydrophobicity of set cement, its water fillable porosity, thermal conductivity under water-saturated conditions, mechanical stability in thermal shock tests with a temperature gradient of 150°C, as well as on pozzolanic reactivity of FCS were considered.

2. MATERIALS AND METHODS

2.1 Stating Materials

Class G well cement (OPC) was supplied by Trabits group, and the X-ray powder diffraction (XRD) data showed that its crystalline composition included four principal phases, hatrurite (ICDD# 04-014-9801, $3CaO.SiO_2$, C_3S), calcio-olivine (ICDD#04-012-6734, $CaO.SiO_2$, C_2S), brownmillerite (#04-007-5261, $4CaO.Al_2O_3$, Fe_2O_3), and calcium sulfate (#01-074-1905, $CaSO_4.2H_2O$). CenoStar Corp. provide the fly ash cenospheres (FCS) under the trade name "CenoStar ES500". The FCS's bulk density is 0.32-0.45 g/cm^3 and TC is 0.1-0.2 W/mK (Sugama and Pyatina 2021). The major crystalline phases of FCS were mullite (ICDD#04-016-1586, $Al_{2.22}$ $Si_{0.78}$ $O_{4.89}$) and silica (#04-008-8437, SiO_2). The cumulative size distribution of FCS was as follows: 3 wt.% 300 µm, 54 wt.% 150 µm, 19.5 wt.% 106 µm, 15 wt.% 75µm, and 8.5 wt.% < 74 µm.

U.S. Silica Corporation provided silica flour with particle size 40-250 µm. XSBR latex was supplied by Cudd Energy Services. Table 1 shows oxide compositions of the starting materials.

Table 1. Oxide compositions of the starting materials

Component	Oxide composition, wt%							
	Al_2O_3	CaO	SiO_2	Fe_2O_3	Na_2O	K_2O	TiO_2	SO_3
Class G cement	3.0	67.6	18.4	3.9	0.3	1.3	-	5.5
Silica flour	-	-	100	-	-	-	-	-
FCS	35.0	2.7	50.1	7.1	0.30	3.1	1.6	-

2.2 Samples preparation

The samples were prepared by dry blending OPC, FCS, silica flour. The XSBR latex was added to the mix water prior the mixing with the dry blend. The dry blend consisted of 38 % OPC, 38 % FCS, 24 % silica flour by weight. To determine the content of solid polymer (P) in XSBR latex, the latex was dried for 3 days in an oven at 100^{0}C until it reached a constant weight, the measured composition was ~43 wt% P and ~57 wt% water. Three different concentrations of XSBR latex were used for P /Composite (C) slurries 5, 15, and 25 wt%. The total water (W, added water + water in latex)/C ratios were 0.51, 0.45, 0.37, and 0.31 for 0, 5, 15, and 25% P/C formulations respectively. The slurries were prepared by adding water with latex to the dry blend and mixing by hand for a minute. Slurries were pored into different molds for different types of tests, left for 24 hours at room temperature. Then the hardened composites were demolded and placed in a 99 ± 1% relative humidity for 24 hours at 85°C; finally, the composites were autoclaved in non-stirred Parr Reactor 4622 for 24 hours at 100°C.

2.3 Measurements

The slump size of the slurries, mm, was measured using a 40 mm high polyethylene cone with the dimension of the hole at the top of 20 mm in diam., and at the bottom of 45 mm in diam. The cement slurry was filled in the cone placed on a flat carbon steel plate. Thereafter, the cone was slowly lifted, allowing slurry to flow out. The diameter of the spread slurry, mm, was measured 20 seconds later.

For the TS tests the 100°C-autoclaved samples were heated for 24 hours in an oven at 175°C and then immersed into 25°C water. This heat-quenching process was repeated three times. The extent of TS resistance was evaluated from the changes in mechanical properties and thermal conductivity after TS.

Attenuated Total Reflectance-Fourier Transform Infrared Spectroscopy (ATR-FTIR, Perkin Elmer Spectrum 100) and x-ray diffraction measurements (40 kV, 40 mA copper anode X-ray tube) were used for samples characterization before and after the TS tests. The PDF-4/Minerals 2021 database of International Center for Diffraction Data (ICDD) was used for analyses of XRD patterns.

To assess water-repellent property of cured composites, contact angle measurements for water droplet on air-dried composite surfaces were done with Model CAA 3, Imass Inc., using rectangular prism samples (15 mm x 75 mm x 2 mm). Prior to these measurements, all samples were left open to the air at room temperature for 7 days to prepare air-dried surfaces. Each contact angle value is an average of the measurements performed at five different locations.

To evaluate composites' water repellency, the water-fillable porosity of cylindrical water-saturated samples (20 mm diam. x 40 mm high) after curing in 100°C autoclave was computed by W_{wet}-W_{dry}/W_{wet} x 100, where W_{wet} is the weight of water-saturating sample and W_{dry} is the weight of sample dried for at least 4 days in a vacuuming oven at 65°C until the weight of the sample does not change anymore.

The TC was measured by Quick Thermal Conductivity Meter, OTM-500, Kyoto Electronic on rectangular prism samples (60 mm x 120 mm x 20 mm) using water-proofed probe consisting of a single heater and thermocouple. The probe was placed on cement surface after extra water was removed from the water-saturated cement surface with paper towel.

Unconfined compressive strength, Young's modulus, and compressive fracture toughness measurements were performed on cylindrical samples (20 mm diam. x 40 mm high) using Electromechanical Instron System Model 5967. The compressive toughness was determined from the area under the compressive stress-strain curve. The ideal fracture toughness is achieved for an adequate balance between compressive strength and ductility.

JEOL 7600F Scanning Electron Microscope image analysis coupled with Energy Dispersive X-ray (EDX) elemental composition measurements on freshly broken cement samples was employed for morphological analyses and phase identifications.

3. RESULTS AND DISCUSSIONS

3.1 Slurry properties

The densities and slump size of the slurries with different polymer-to-composite ratios are given in Table 1. XSBR has a strong dispersing effect on the OPC slurry. Even with the decrease of W/C ratio from 0.51 for the neat slurry to 0.31 for 25% XSBR the size of the slump increased from 60 to 75 mm due to increased slurry fluidity. Another XSBR effect is decrease of the slurry density due to the air entraining in the presence of the polymer. The slurry density drops from 1.26 to 1.04 for slurries with 0 and 25% XSBR respectively. Note that an antifoaming agent was not used in the blends.

The data show that XSBR improves the workability/pumpability of the slurry.

Table 1: Properties of composite slurries with different XSBR latex weight percent.

Property	P/C ratio, %			
	0	5	15	25
Water-to-composite ratio (W/C)	0.51	0.45	0.37	0.31
Density, d/cm^3	1.26	1.11	1.06	1.04
Sump size, mm	60	64	72	75

3.2 Crystalline phase compositions

The crystalline phase compositions of 100°C autoclaved OPC-based composites with and without XSBR are shown in Figure 1. Peaks of the same crystalline phases can be found in both patterns for the most part. The patterns differ in the intensity of 1) portlandite peaks, 2) carbonate peaks, and 4) peaks of non-reacted cement phases. The higher intensity of the peaks from the original crystalline OPC phases (calcio-olivine and brownmillerite) in the sample with 25% XSBR latex suggests that the polymer slows down cement hydration. As a result, there is still gypsum present in XSBR latex-modified cement but not in the neat sample. Latex also prevents sample's carbonation – peaks of carbonated phases are significantly lower in latex-modified cement than in the control. The results were similar for the slurries autoclaved at 175°C (Figure 2). One of the possible explanations is polymer-calcium interaction preventing formation of calcium carbonates. There were no peaks of crystalline calcium-silicate hydrates after both curing temperatures, which means that they mostly remain amorphous after the short-time curing of 24 hours.

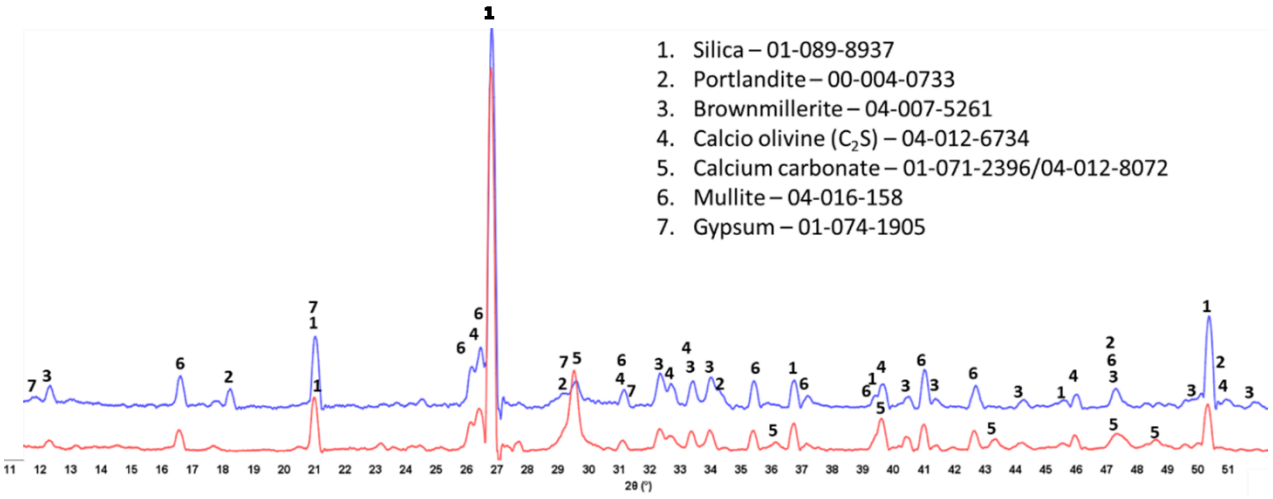

Figure 1: XRD patterns of 100°C-autoclaved OPC composites modified (Blue) and unmodified (Red) with XSBR.

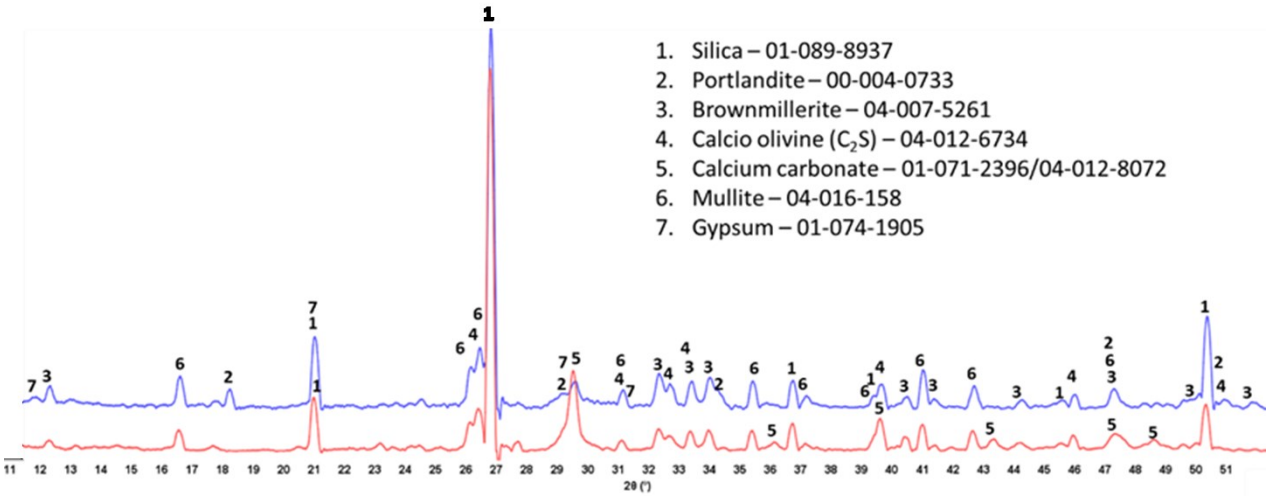

Figure 2: XRD patterns of 175°C-autoclaved OPC composites modified (Blue) and unmodified (Red) with XSBR.

3.3 Infrared analyses of cement composites before and after the TS tests

Figure 3 depicts ATR-FTIR spectra in frequency range of 2000 to 650 cm^{-1} for control and latex-modified 100°C-autoclaved composites before and after the TS tests. The control composite displayed peaks relevant to $CaCO_3$ (1497, 1426, 872 cm^{-1}) and C-S-H (960 cm^{-1}) before TS tests. The intensity of carbonate peaks strongly increased after the TS. On the other hand, carbonation for both of 25% P/C-modified composites before and after TS was very low. The peak at 960 cm^{-1} related to latex decreased in TS treatment, at the same time, this composite showed peaks related to calcium carboxyl that increased after three 175°C heat → 25°C water quenching cycles. This was a result of latex partial degradation with formation of additional calcium-carboxylate complexes adsorbing on the solid particles. These results are in agreement with the XRD data. Presence of latex abated sample carbonation both before and after the TS tests.

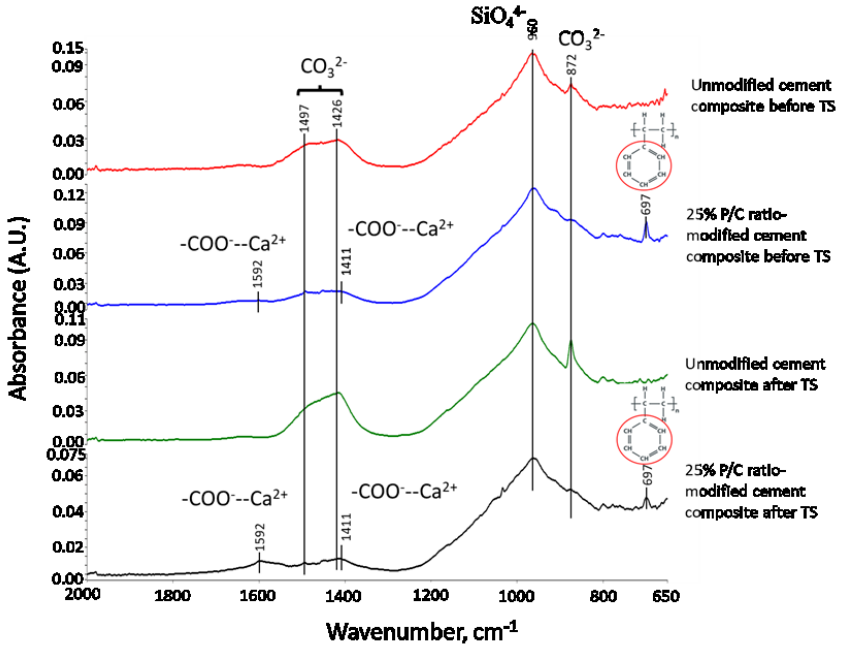

Figure 3: ATR-FTIR spectra of 25% P/C ratio-modified and control OPC composites before and after TS test.

3.4 Analyses of morphological alterations of the samples

The analyses of samples' morphologies were performed to evaluate effect of XSBR latex on pozzolanic reactions of FCS. Figure 4 shows typical freshly broken surfaces of control and latex-modified (25% P/C) samples autoclaved at 100°C. The samples were coated with Ag to avoid charging effects. The images of the control sample (top left) show strong degradation of FCS in pozzolanic reactions. The hard shells of FSC particles are broken, their inner surfaces are covered with the pozzolanic reactions products. As a result of FCS shells damage their insulating function is lost. The damage of FCS also negatively affects mechanical and water repellant properties of the cement creating weaker porous structure.

The elemental composition in the marked area of the cement matrix away from FCS (top left) includes Ca, Si, C, and O as major elements and Fe, S, Al, and Mg as minor ones. The C/Ca, Al/Ca, and Si/Ca atomic ratios are 2.00, 0.28, and 0.99, respectively. Thus, the matrix seems to be constructed by mainly C-S-H, CH, and calcium carbonate. The morphology of modified composite (bottom left) differed noticeably from unmodified one. The FCS shells remained intact, clearly demonstrating that XSBR latex adequately protected the FCS shell against pozzolanic reaction-led erosion. Consequently, FCS insulating properties, strength, and water repellency persist through the HT autoclaving. The atomic ratios in the selected area were: 5.16 C/Ca, 0.08 Al/Ca, and 0.66 Si/Ca. Compared with that of unmodified one, there were two major differences: one was a very high quantity of C; the other is considerably lower Al and Si contents. The carbon belongs to the latex and the calcium carboxylate complexes.

The FCS surfaces of the control sample (top right) are covered with the products of pozzolanic reactions. The original FCS are aluminum-silicates (mullite) with silica. As is evident from 0.86 Si/Ca and 0.14 Al/Ca atomic ratios, the reaction products of pozzolanic degradation may be C-S-H and calcium aluminate silicate ($CaO.Al_2O.SiO_2.H_2O$, C-A-S-H). The FCS surfaces of the modified composite (bottom right) were smooth without any pozzolanic reaction products. EDX indicated 5.87 C/Ca, 0.71 Al/Ca, and 1.77 Si/Ca ratios. This C/Ca ratio was nearly 3-fold higher than that of the control. Furthermore, the values of Al/Ca and Si/Ca ratios were equivalent to ~5- and ~2-times higher than for the control sample. Hence, since Al and Si come from underling FCS surfaces, a possible explanation is that this smooth surface area of FCS was covered with Ca-latex complexes (high carbon content on the surface and presence of Ca), which protected it from pozzolanic degradation.

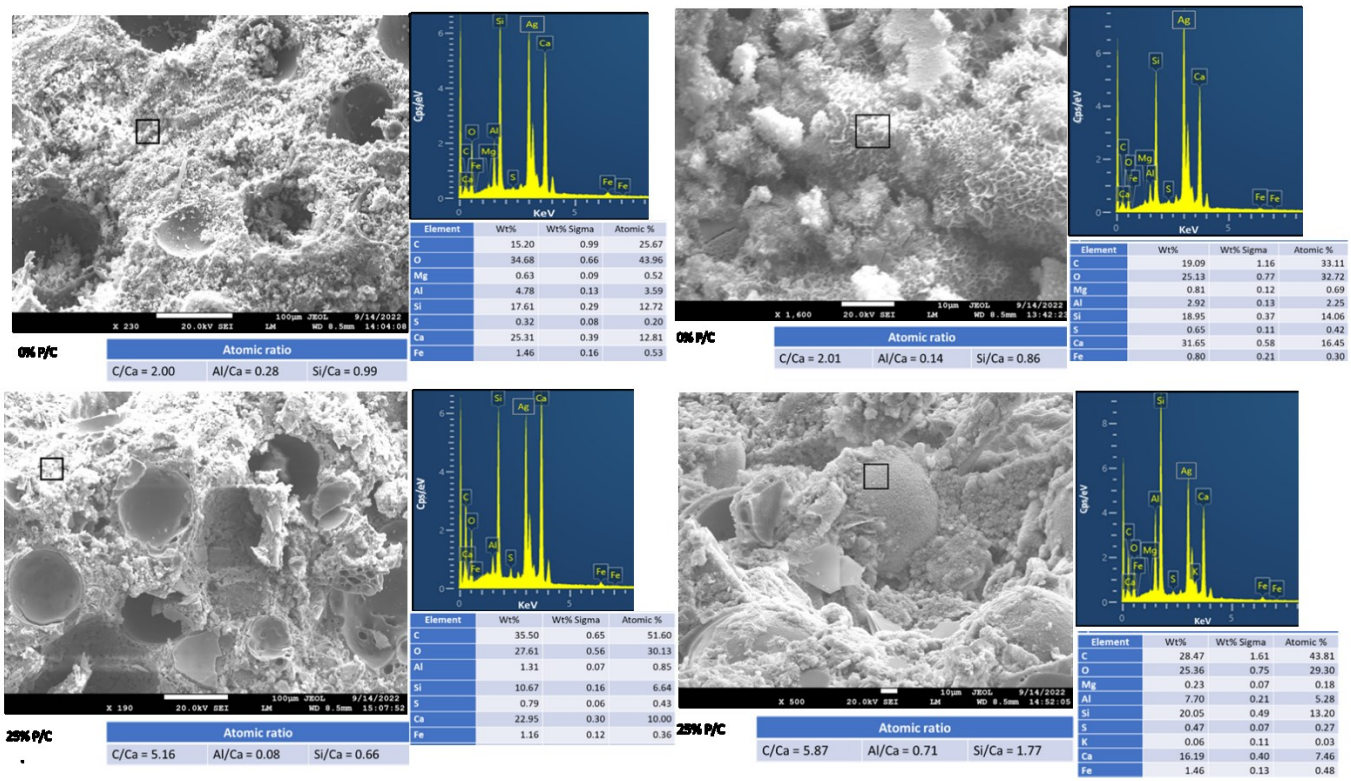

Figure 4: Comparison of morphological features of control (top) and XSBR-modified (bottom) 100°C-autocalved OPC composites.

3.5 Water-fillable porosity and water-repellency

Water fillable porosity of the 100°C-autoclaved composites with varied XSBR latex content before and after the TS is shown in Figure 5. The porosity also decreased with the increased latex content. The porosity of 38.9 % for 0% P/C dropped by ~30% to 27.3% for 25% P/C. After TS, the porosity of all samples declined. This decline was more important for modified samples. Particularly, the 15 and 25% P/C samples exhibited porosity reduction of >50%. Latex addition was clearly beneficial for reducing the samples' water-fillable porosity. This agrees with the conclusions of morphological analyses that showed decreased degradation of FCS in latex-modified composites and reduced samples' porosity.

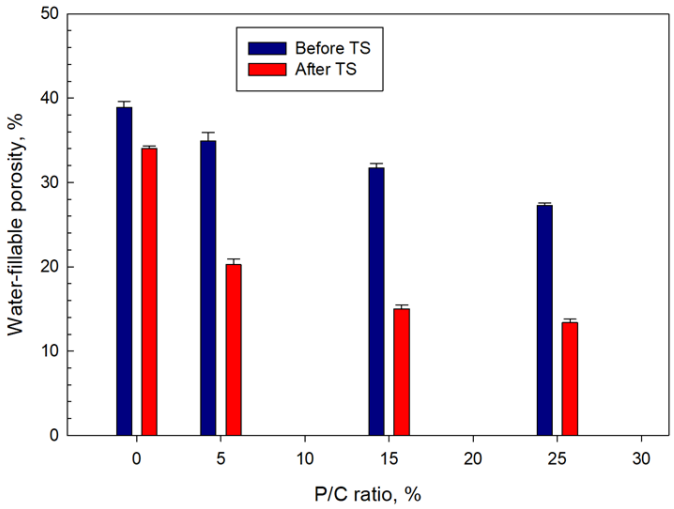

Figure 5: Water-fillable porosity of control and 5, 15, and 25% P/C ratio-modified composites before and after TS.

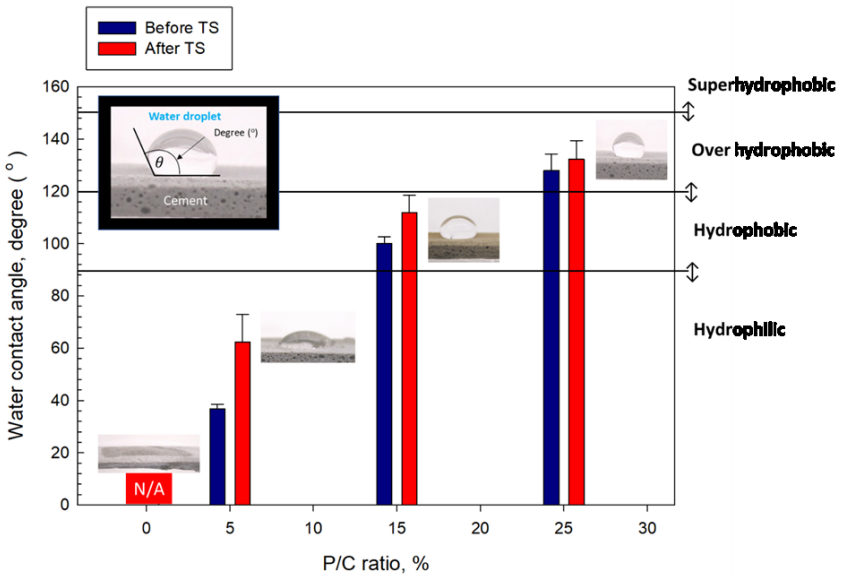

Figure 6: Changes in the surface hydrophobicity (measured by the water droplet contact angle) for control and 5, 15, and 25% P/C ratio-modified composites before and after TS.

Figure 6 shows increasing water-repellency of composites' surfaces with the increase of latex content. As the concentration of the latex increases the surface becomes more hydrophobic with improved water repellency. At low, 5% latex content the surface of the composite remains hydrophilic, at 10% latex content it becomes hydrophobic, and at 25% latex it can be classified as over hydrophobic. Improved water repellency of the surface helps to reduce water penetration into the cement decreasing water-fillable porosity of the samples and affecting their thermal conductivity under water-saturated conditions.

3.6 Thermal-conductivity

Figure 7 shows the changes in thermal conductivity, TC, as a function of P/C ratio before and after the TS. Before TS, TC (0.42 W/mK) of 0% P/C decreased with increasing P/C ratio down to 0.39, 0.35, and 0.32 for 5, 15, and 25 % P/C ratio, respectively. This result was due to the improved water-repellency, decreased water-fillable porosity, and decreased slurry density with increased latex content. The property of high hydrophobicity leads to minimum water ingress. Along with the insulative air bubbles entrained by latex into the slurries these properties help to reduce TC of water-saturated composites. TS tests resulted in further considerable decrease in TC. For instance, 15 and 25% P/C ratio samples with 0.25 and 0.23 W/mK, respectively, was tantamount to ~29 and ~28 % reduction compared with that of the samples before TS made with the same P/C ratios. By contrast, TC of the control (P/C 0%) dropped by only 7% after the TS tests.

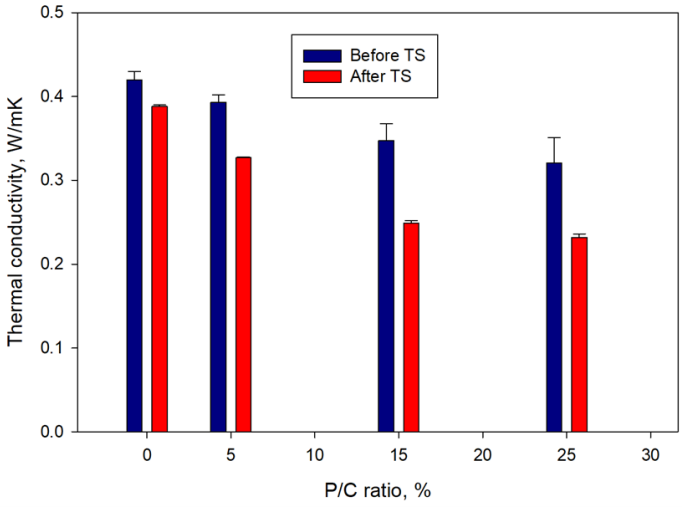

Figure 7: Thermal conductivity of XSBR-modified and unmodified OPC composites before and after TS.

3.7 Mechanical properties

Figure 8 shows the compressive strength and the rate of its decline in TS tests for composites with different P/C ratios. Increase of latex concentration resulted in stronger cements. Before the TS, the composite made with 25% P/C had the compressive strength of 16.6 MPa, which was ~75% higher than that of the control. After the TS, all composites lost some strength. The control composite lost 26.8% in strength compared after the TS. The rate of the strength reduction for XSBR-modified composites depended on P/C ratio. The increase in P/C ratio led to a lower strength decline in TS tests. The 5, 15, and 25% P/C ratio samples displayed the loss of 20.2, 16.5, and 14.4 % of the strength, respectively. Compared with the control, the 15 and 25% P/C composites experienced ~38 and ~46% lower strength loss. The data demonstrate that XSBR clearly improves composites resistance to TS.

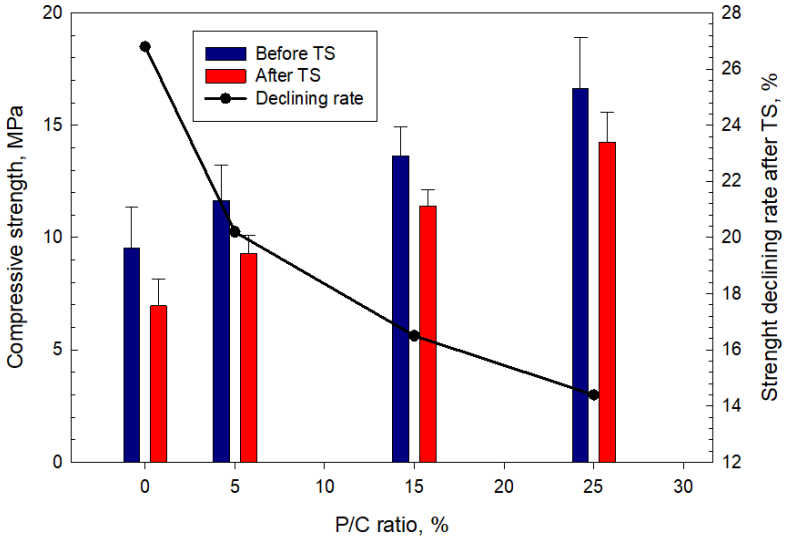

Figure 8: Compressive strength and strength decline rate after the TS tests for the control and XSBR-modified composites.

The Young's modulus (YM) data mirrored those for the compressive strength (Figure 9) with the modulus increasing at higher latex concentrations. YM value of 859 MPa for control increased by ~37% to 1176 MPa for 25% P/C. After TS, the decline in YM ranged from ~24% for the control to ~13% for 25% P/C compared with the values before the TS. The composites with high latex contents exhibited a lower decline rate of stiffness. The loss in stiffness for all composites implied that the composites underwent ductile to soft transition during the TS tests. The 25% P/C composite sustained the ductility with minimal transition to softness.

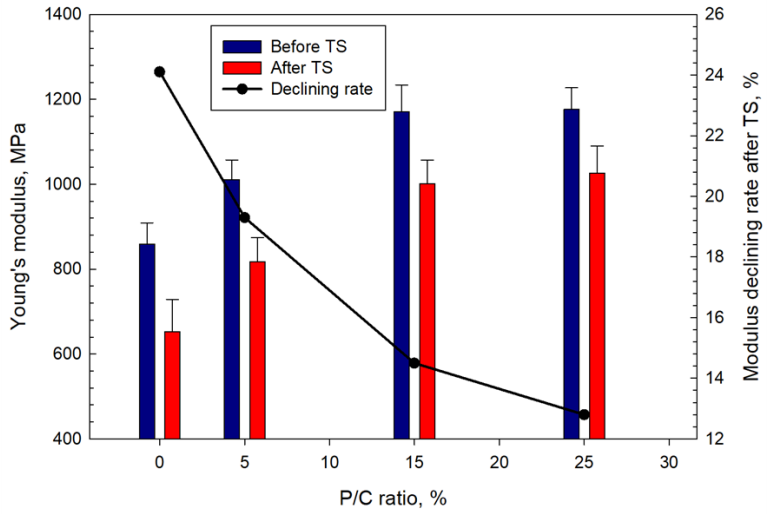

Figure 9: Young's modulus and its decline rate after the TS tests for the control and XSBR-modified composites.

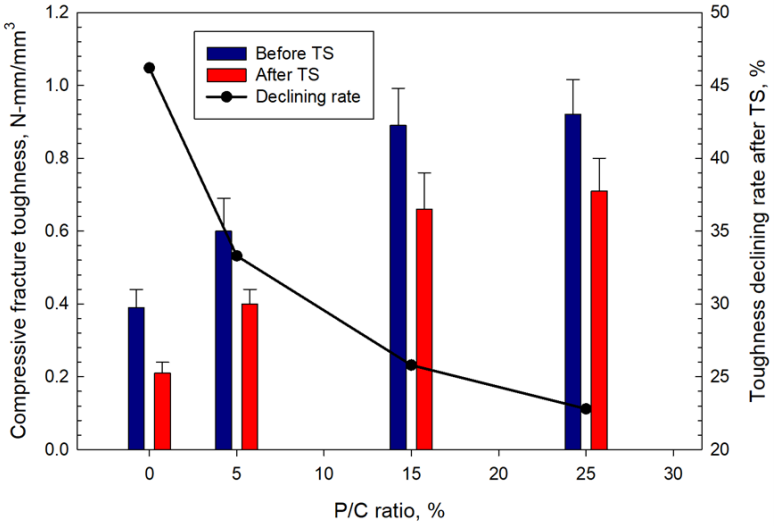

Figure 10: Compressive toughness and its decline rate after the TS tests for the control and XSBR-modified composites.

The compressive fracture toughness increased with the increase of latex concentration. The 0.39 N-mm/mm^3 toughness of 0% P/C was enhanced by ~2.4-fold to 0.92 N-mm/mm^3 for composite made with 25% P/C ratio. Since the toughness refers to the combination of ultimate strength and ductility of composites, the addition of XSBR improved this combination. Like the strength and YM trends, all samples lost some of the toughness in TS tests. The toughness decline rate decreased with increasing P/C ratio. The 0, 5, 15, and 25% P/C ratios corresponded to ~46, ~33, ~26 and ~23% toughness decline rate respectively.

The data on mechanical properties of tested composites demonstrate that addition of high concentrations of XSBR latex improve strength and ductility of the composites and their TS resistance under the test conditions.

All the evaluations of the control and XSBR latex-modified composites demonstrated improved composites performance, including mechanical properties, water-repellency, and insulating nature, with the addition of high concentrations of the polymer.

CONCLUSIONS

XSBR latex, which is terpolymer of polystyrene (PS), polybutadiene (PB), and polyacrylic acid (PAA), was evaluated as potential additive for designing hydrophobic thermally insulating, thermal shock-resistant Class G well cement (OPC) composites containing fly ash cenospheres (FCS). The composites were tested at thermal gradient of 150°C for applications in thermal energy storage system wells with temperatures between 100° and 175°C. At 100°C hydrothermal temperature carboxyl groups within PAA reacted with Ca^{2+}, liberated from hydrolysis of OPC creating Ca^{2+}-coordinated PAA chelate complex in the polymer. At higher temperature of 175°C additional carboxyl groups formed resulting in more calcium complexation and polymer adsorption on hydrating cement surface. The chelated calcium polymer improved performance of OPC-based composites in TS tests (three cycles of 150°C temperature gradient; one cycle: 175°C heat → 25°C water quenching). Ca complexation also contributed to the following performance factors: 1) eliminating the carbonation of OPC; 2) controlling the hydration reactions of OPC; 3) enhancing composites' extent of hydrophobicity; 4) decreasing water-fillable porosity; 5) reducing thermal conductivity of water-saturated composites; 6) minimizing the loss of compressive strength, Young's modulus as stiffness, and compressive fracture toughness in TS tests; and 7) abating the pozzolanic activity of FCS.

The measurements of water repellency, estimated by water-droplet contact angle (°) on OPC composite surfaces, demonstrated that 25% Polymer/Composite (P/C) -modified surfaces before and after TS fell into the over hydrophobic range of >120° to 150°, compared with hydrophobic classification of ≥90°-120° for 15% P/C, and hydrophilic of < 90°C for 5% and 0% P/C composites. The low water-permeability was measured for the modified composites compared to the control samples: before TS it was 38.9% for 0% P/C and 27.3% for 25% P/C. After TS, the porosity of all XSBR-modified composites was considerably reduced, for instance, the porosity of pre-TS 25% P/C decreased by nearly 50% to 13.4%, compared with only 13% reduction for the control. The combination of excellent water repellency and waterproofing led to a low TC, thereby resulting in good thermal insulating performance of water-saturated composites. The data for TS samples exposed to TS tests showed that 0.39 W/mK of the control sample was ~40% higher than 0.23 W/mK for 25% P/C. The TS resistance of the composites was judged by the decline rate of their mechanical properties in TS tests. For 25% P/C composite, the decline rate of compressive strength, stiffness, and fracture toughens was as low as 14.4%, 12.8%, and 22.8%, respectively, compared with 26.8%, 24.1% and 46.2%, respectively, for the control. Thus, XSBR offered a good thermal shock resistance to OPC-based formulations. Finally, XSBR latex provided protection of hard water-impermeable aluminosilicate shell structure of hollow FCS microspheres against pozzolanic reaction-led erosion. The morphological exploration coupled with elemental composition analyses revealed that in 100°C-autclaved 25% P/C composite, the surfaces of FCS were covered with calcium-chelated polymer ensuring an adequate protection of FCS. In addition, XSBR acted as a dispersant improving slurries workability and pumpability. It also decreased the density of the slurries resulting in better insulating properties

Based on the above information we conclude that XSBR-modified OPC-based composites have a good potential for the use as hydrophobic thermal insulating, thermal-shock resistant well OPC composites in geothermal energy storage systems up to 175°C.

ACKNOWLEDGMENTS

This project has been subsidized by GTO EERE under the auspices of the US DOE, Washington, DC, under contract No. DE-AC02-98CH 10886). Research was carried out in part at the Center for Functional Nanomaterials, Brookhaven National Laboratory, which is supported by the US Department of Energy, Office of Basic Energy Sciences, under Contract No. DE-SC0012704.

REFERENCES

Barluenga, G. 2010. "Fiber-Matrix Interaction at Early Ages of Concrete with Short Fibers." *Cement & Concrete Research* 40: 802–9.

Butler, M, S Hempel, and V Mechtcherine. 2011. "Modelling of Ageing Effects on Crack-Bridging Behavior of AR-Glass Multifilament Yarns Embedded in Cement-Based Matrix." *Cement & Concrete Research* 41 (4): 403–11.

Castricum, HL, A Sah, R Kreiter, DHA Blank, JF Vente, and JE ten Elshof. 2008. "Hydrothermally Stable Molecular Separation Membranes from Organically Linked Silica." *Journal of Materials Chemistry*, no. 18: 2150–58. https://doi.org/DOI https://doi.org/10.1039/B801972J.

Koyano, KA, T Tatsumi, Y Yanaka, and S Nakata. 1997. "Stabilization of Mesoporous Molecular Sieves by Trimethylsilylation." *Journal of Physical Chemistry B* 101: 9436–40.

McIvor, SD, MI Darby, GH Wostenholm, B Yates, L Banfield, R King, and A Webb. 1990. "Thermal Conductivity Measurements of Some Glass Fibre- and Carbon Fibre-Reinforced Plastics." *Journal of Materials Science* 25: 3127–32.

Park, DH, N Nishiyama, Y Egashira, and K Ueyama. 2001. "Enhancement of Hydrothermal Stability and Hydrophobicity of a Silica MCM-48 Membrane by Silylation." *Industrial Engineering Chemical Research* 40 (26): 6105–10. https://doi.org/https://doi.org/10.1021/ie0103761.

Sugama, Toshifumi, and Tatiana Pyatina. 2013. "Functional Acrylic Polymer as Corrosion Inhibitor of Carbon Steel in Autoclaved Air Foamed Sodium Silicate-Activated Calcium Aluminate/Class F Fly Ash Cement." *Engineering* 5: 887–901.

Sugama, Toshifumi, and Tatiana Pyatina. 2021. "Hydrophobic Lightweight Cement with Thermal Shock Resistance and Thermal Insulating Properties for Energy-Storage Geothermal Well Systems." *Materials* 14: 6679.

Sugama, Toshifumi, and Tatiana Pyatina. 2022. "Thermally Insulating, Thermal Shock Resistant Calcium Aluminate Phosphate Cement Composites for Reservoir Thermal Energy Storage." https://doi.org/10.3390/ma15186328.

Verma, A., and Pruess, K.: Enhancement of Steam Phase Relative Permeability Due to Phase Transformation Effects in Porous Media, Proceedings, 11th Workshop on Geothermal Reservoir Engineering, Stanford University, Stanford, CA (1986). <Reference Style>

Wang, C.T., and Horne, R.N.: Boiling Flow in a Horizontal Fracture, Geothermics, 29, (1999), 759-772. <Reference Style>